

# Anomalous suppression of spin-exchange relaxation in alignment signals in cesium in ultra-weak magnetic fields

M.V. Petrenko<sup>1</sup> and A.K. Vershovskii<sup>1</sup>

<sup>1</sup>*Ioffe Institute, Russian Academy of Sciences, St. Petersburg, 194021 Russia*  
e-mail address: antver@mail.ioffe.ru

The results of a study of the dynamics of atomic moments alignment in cesium under optical pumping by linearly polarized resonant light in a transverse magnetic field are presented. It is shown that there are alignment components whose relaxation does not depend on spin-exchange broadening. The effect of suppression of spin-exchange relaxation in zero magnetic fields is detected, which is similar in its manifestations to the SERF (Spin-Exchange Relaxation Free) effect observed in orientation signals. This observation is interesting from the standpoint of general theory, since the law of conservation of angular momentum responsible for maintaining orientation in the SERF mode should not guarantee the preservation of alignment under the same conditions. A comparison with theoretically calculated parameters of SERF resonances in orientation is given. A qualitative explanation of the observed effect is presented.

**Keywords:** optically detected magnetic resonance, magnetic moment of an atom, optical pumping, alignment, relaxation, law of conservation of angular momentum.

## 1. Introduction

Various quantum sensors based on the effects of optical pumping in atoms (primarily hydrogen-like alkalis) and atom-like structures, such as nitrogen-vacancy (NV) color centers in diamond, have become among the most rapidly developing and sought-after devices in applied physics in recent decades. These include atomic clocks [1,2], sensors of magnetic field [3–5], rotation (gyroscopes) [6,7], temperature [8], electric field strength [9], etc.

The vast majority of alkali atom sensors are based on the optical orientation effect. Orientation is usually understood as both the process and the result of the action of a circularly polarized beam resonant to an optical atomic transition on an ensemble of atoms; in this case, the angular momentum is transferred from photons to the atoms, and a group kinetic and magnetic moment is formed. In the hierarchy of moments, orientation is a first-order moment. It is characterized by an asymmetric distribution of the populations of the Zeeman sublevels, and, as a consequence, a nonzero value of the average moment.

For a long time, the main obstacle to the creation and then increase of sensitivity of optical quantum sensors was the rapid relaxation of oriented atoms during collisions both with the cell walls and with each other (in solid-state sensors – spin-lattice and spin-spin relaxation). It is very important to note that relaxation processes are closely related to conservation laws, primarily – with the law of conservation of angular momentum. Thus, due to this law, spin-exchange processes do not change the total angular momentum of the atomic ensemble. This is why they do not contribute to the relaxation of the longitudinal component of the total moment with respect to the magnetic field – that is, to the longitudinal (determined by time  $T_1$ ) relaxation of orientation. At the same time, these processes are capable of changing the phases of the precession of colliding atoms,

while preserving the total moment. This determines the contribution of spin-exchange to the transverse (determined by time  $T_2$ ) relaxation. Note that in classical magnetic resonance described by stationary Bloch equations, the resonance width is determined by the time  $T_2$ . Therefore, it is transverse relaxation that limits the achievable sensitivity of quantum sensors. This fully applies to SERF sensors based on the level crossing (Hanle) resonance [10] in zero magnetic field.

Methods for suppressing relaxation on the cell walls were soon found: filling the cell with buffer gases [11] that slow down the motion of atoms, or applying anti-relaxation coatings [12]. Later, W. Happer showed [13] that spin-exchange relaxation can also be partially or completely suppressed under conditions where most of the colliding atoms are in identical states. This subsequently led to a real breakthrough in quantum magnetometry: SERF zero-field sensors were created [14,15], and then non-zero-field sensors using "stretched" states [4,16,17]. These methods of suppressing spin-exchange relaxation are also based on conservation of angular momentum: in an ensemble in which all atoms have the same (maximum in modulus) projection of angular momentum and a common phase of precession, a change in this state is impossible without changing the total angular momentum and its projection. In particular, the SERF effect, which ensures almost complete suppression of spin-exchange relaxation, is due to the conservation of the total angular momentum of both hyperfine sublevels, which due to ultra-frequent collisions precess at a certain common frequency [18].

All these considerations, however, turn out to be useless in the case of alignment, since it is characterized by a zero value of the average moment. Alignment is a second-order moment in the hierarchy. It arises when atoms are pumped by linearly polarized or unpolarized light; it is characterized by a symmetric distribution of the populations of the

Zeeman sublevels. Quantum magnetic field sensors based on alignment, despite their smaller distribution, are characterized by certain advantages, such as the absence of dead zones [19,20], reduced orientation error [21,22], small drift, and metrological accuracy over long observation times [23]. It is interesting to note that sensors based on NV centers use a mechanism of pumping by unpolarized radiation, which creates alignment in the NV ensemble.

A theoretical description of the alignment effects in alkali metals for stationary cases is given in [24,25], and developed in detail for quasi-stationary cases in [26]. The idea of a zero-field magnetometer based on the alignment effect, which is attractive due to the extreme simplicity of the optical scheme [27], is also developed in [26,28].

At the same time, it can be confidently stated that the potential of quantum alignment sensor circuits has not yet been fully revealed. Thus, in [26], a cell with a paraffin coating was investigated. Such coatings retains their properties at relatively low (below 70°C) temperatures. Signals in such cells are characterized by extremely small widths [29], but also, as a consequence of low concentrations of atomic vapors, by relatively small amplitudes. In addition, cells with anti-relaxation coatings are very difficult to compactify. Therefore, in our work, signals were investigated in a compact (5×5×5 cm<sup>3</sup>) cell with high buffer gas pressure – in such cells, the SERF effect on orientation is realized.

A rigorous definition of orientation, alignment, and higher-order moments is given within the framework of the so-called  $\kappa\eta$ -representation [30,31], based on the expansion of the momentum distribution in irreducible spherical operators. The convenience of the  $\kappa\eta$ -representation is that the dynamics of each of the multipoles into which the momentum distribution in the ensemble is decomposed can be described independently of the other multipoles. In particular, the second-order moment is characterized by five multipoles  $\rho_{-i}^{(2)}$  ( $i = -2 \dots 2$ ), each of which, in turn, can be characterized by its own relaxation rate. In the steady state, of these multipoles, only the multipole  $\rho_0^{(2)} \sim \langle 3F_z^2 - F^2 \rangle$ , which is responsible for the population distribution [32] (p. 375), is non-zero – it is usually called the “alignment”. It is this multipole that is created and detected by linearly polarized pump light.

Let us consider a hydrogen-like atom with a nuclear spin  $I$ . The ground state of such an atom is split into two hyperfine levels with total moments  $F = I \pm 1/2$ , corresponding to two possible projections of the electron spin onto the nuclear spin. In a magnetic field, each hyperfine level is split into  $2F + 1$  sublevels with projections of the magnetic moment  $m_F = -F \dots F$ , characterized by relative populations  $n_{mF}$ . Then in a simple

three-level system with  $I = 1/2$  and  $F = 1$   $m_F = -1, 0, +1$ , and

$$\rho_0^{(2)} = \frac{1}{\sqrt{6}}(n_{-1} - 2 \times n_0 + n_{+1}) \quad (1)$$

Similar expressions can be derived for other values of  $I$ . It is easy to verify that in the equilibrium state  $\rho_0^{(2)} = 0$ . The maximum value of  $|\rho_0^{(2)}|$  is realized in two cases: *i*) all atoms are equally distributed over the levels  $m_F = \pm F$  ( $n_{-F} = n_{+F} = 1/2$ ) and *ii*) all atoms are concentrated at the level  $m_F = 0$  ( $n_0 = 1$ ). The first case corresponds to the maximum positive alignment, the second to the maximum negative alignment. A theoretical study of the relaxation rates of moments of different multipolarity was carried out by W. Happer in [33]. It was shown, for example, that as a result of identical dipole perturbations, the quadrupole moment (i.e. alignment) relaxes three times faster than the dipole moment. But Happer considered atoms as an open system under external influence. In the context of this work, we are interested in relaxation in a closed system under the influence of internal factors (spin exchange).

It is clear that in such a system, collisions can destroy the alignment state without violating either the law of conservation of momentum or the selection rules. During collisions, atoms can exchange the directions of the electron spins. As a result of the exchange, the total moment of the system and its projection on the quantization axis are preserved, and the projection of the spin of each electron changes by  $\pm 1$ . Then, due to hyperfine interaction, the moment is redistributed between the electron  $S$  and nuclear  $I$  spins of each atom, and the state of the electron spin is randomized to a significant extent (since  $I \gg S$ ) [18].

Let us consider a system of two identical atoms with moment projections  $m_{F1} = -F$  и  $m_{F2} = F$  (maximum achievable positive alignment). The total moment of such a system, limited by the range  $0..2F$ , depends on the mutual directions of the two moments, and with the highest probability it is equal to zero (this also applies to an ensemble of atoms in a cell in the absence of circularly polarized light). The total projection of the moment onto the magnetic field is also equal to zero. As a result of a collision, the atoms can pass to the levels  $m_{F1} = -F + 1$  and  $m_{F2} = F - 1$ , respectively; then, after randomization of the electron spin, collide again and either return to the previous state, or pass to the levels  $m_{F1} = F + 2$  and  $m_{F2} = F - 2$ , etc. In the case of initially negative alignment, atoms with moment projections  $m_{F1} = m_{F2} = 0$  as a result of a collision can pass to the levels  $m_{F1} = -1$  and  $m_{F2} = 1$ , respectively, etc. In all the cases considered, collisions in the absence of pumping will eventually lead to the restoration of the equilibrium population while maintaining angular momentum.

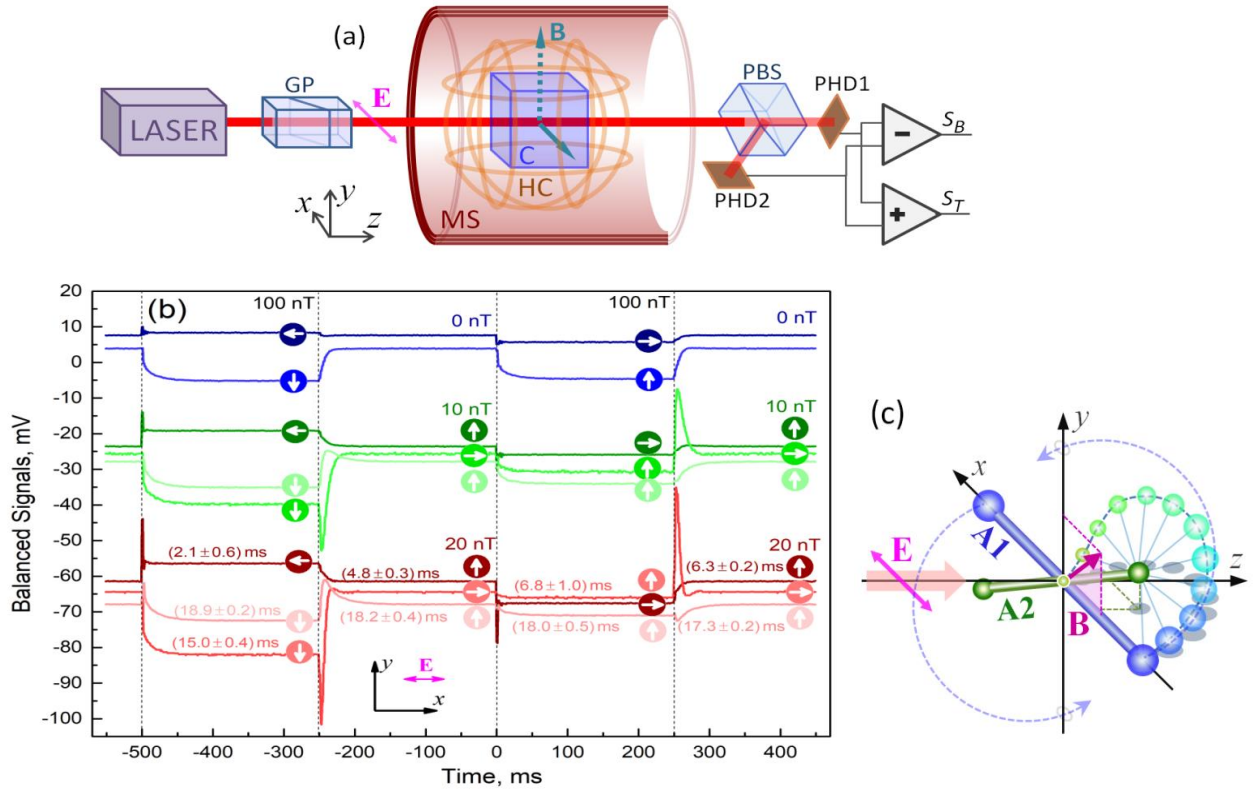


Fig. 1(a) Experimental setup: MS – magnetic shield, PG – Glan prism, HC – Helmholtz coils system, C – cell, PBS – polarization cube, PHD1, PHD2 – photodiodes. The laser frequency stabilization circuit is not shown. (b) Examples of recordings of polarization rotation signals when switching the induction and direction of the magnetic field. The vertical shift is arbitrary. Arrows designate the direction of the magnetic field in the 0xy plane in a given recording interval, the numbers above the arrows are the modulus of the magnetic field induction. Several values of the relaxation times are given. (c) Dynamics of alignment when turning on the ultra-weak field **B** in the XY plane in case of  $T_1 \approx T_2 \approx 1/\omega_L$ . A1 is the initial state of alignment along the  $x$  axis; ten intermediate states are also shown. A2 is the state of alignment in the stationary case at constant pumping and magnetic field; it is obtained by averaging over the intermediate states. The dashed arcs are the hodograph of the precession of alignment in the absence of relaxation.

The obvious conclusion is that spin-exchange relaxation of alignment in a closed system is possible even under the condition of conservation of the total momentum.

Thus, we have no a priori grounds to expect that in the case of alignment, spin-exchange relaxation will not contribute to time  $T_1$ .

For the same reasons, we have no grounds to expect that in zero magnetic fields, the effect of transverse relaxation suppression (time  $T_2$ ) similar to the SERF effect in orientation is realized in alignment.

This is supported by one of our results: under certain conditions, the alignment relaxes significantly faster than the orientation should relax. However, our experimental results also suggest that *i*) in ultra-weak magnetic fields, the alignment relaxes without any contribution from spin-exchange broadening, and *ii*) in zero fields, the alignment can exhibit resonances with a width approximately equal to the width of the ultra-narrow SERF resonances in the

orientation. It follows that the above considerations do not fully describe the relationship between the alignment relaxation and the angular momentum conservation law; it is also possible that the alignment relaxation is related to higher-order angular momentum conservation laws. The remainder of the paper is organized as follows: Section 2 describes the experimental setup, Section 3 presents the experimental results, and Section 4 discusses them.

## 2. Experiment

The experimental setup, previously described in [34], is shown in Fig. 1a. The cell chosen for the study contained, in addition to Cs,  $P_{N2} \approx 300$  torr of buffer gas (nitrogen), which ensured complete mixing of the excited states of Cs. The external cavity laser (VitaWave company) was tuned to the center of the  $F = 4 \rightarrow F' = 3$  transition of  $D_1$  absorption line of Cs (wavelength 895 nm). A Glan prism was used to improve the degree of beam polarization. Below we use a

coordinate system in which the beam propagates along the  $z$  axis, and the electric component of the radiation  $\mathbf{E}$  is parallel to the  $x$  axis.

The cell was placed in a thermostat (not shown in the scheme), which in turn was placed in the center of a multilayer magnetic shield. The residual magnetic field was compensated by the coils of the three-coordinate Helmholtz system using the criterion of the absence of the beam polarization rotation, i.e. up to the light shift of the magnetic levels in the system. The alignment signals were detected by a balanced photodetector, which allowed both the total ( $S_T$ ) and the differential ( $S_B$ ) signals to be simultaneously recorded. These signals are related to the intensities of radiation polarized along the  $x$  and  $y$  axes as follows:

$$\begin{aligned} I_x &= \frac{1}{2} \left( S_T + \sqrt{S_T^2 - S_B^2} \right) \\ I_y &= \frac{1}{2} \left( S_T - \sqrt{S_T^2 - S_B^2} \right) \end{aligned} \quad (2)$$

The  $S_T$  signal characterizes the intensity of light passing through the cell. The  $S_B$  signal is determined by the angle  $\Delta\varphi = \varphi - \varphi_0$  of rotation of the beam polarization plane:

$$S_B = -\frac{I}{2} \sin(2\Delta\varphi) \quad (3)$$

The beam rotation in the case of alignment is due to the effect of linear dichroism [34]. For  $\Delta\varphi \ll 1$ , which is almost always the case for dichroism signals,  $S_B \sim \Delta\varphi$ . The coefficient of conversion of the photocurrent into the output voltage of the photodetector (shown below in the graphs) was  $5 \times 10^3$  V/A.

The results shown in Fig. 1b and Fig. 2 were obtained at a cell temperature of  $T_c = 120^\circ\text{C}$ . The calculated parameters at this temperature are as follows: the atomic concentration is  $4.75 \times 10^{13} \text{ cm}^{-3}$  [35], the spin-exchange relaxation rate is  $47 \times 10^3 \text{ s}^{-1}$  [36], and the linewidth of the magnetic resonance orientation, taking into account the nuclear slowdown factor at strong pumping, is approximately 1.6 kHz or 460 nT [37]. The corresponding time constant is  $\sim 0.1$  ms. The magnitude of the longitudinal broadening can be estimated at (5–10) Hz, or (1.75–3.5) nT.

Fig. 1b shows the records of  $S_B$  signals registered when switching on and off the transverse field  $B_{\text{Mod}} = |\mathbf{B}_{\text{Mod}}| = 100$  nT. In the records, one can distinguish sections corresponding to fast transient processes and sections with slow (units and tens of ms) relaxation. This relaxation time is 1–2 orders of magnitude longer than the spin-exchange relaxation time, and by order of magnitude corresponds to the calculated times  $T_1$  without taking into account the light broadening.

In order to reduce the amplitudes of transient processes, we replaced the periodic switching on and off of the field by changing its direction. Due to the symmetry of the alignment, changing the direction of the field to the opposite while maintaining its modulus does not affect the

system; response signals can only be obtained in the presence of the bias field  $\mathbf{B}_{\text{Offs}}$ . We investigated such signals by varying  $\mathbf{B}_{\text{Mod}}$  and  $\mathbf{B}_{\text{Offs}}$ , and in addition to switching the field direction to the opposite ( $X$ - $X$  and  $Y$ - $Y$ ), we used (as in [34]) a change in the direction of the  $\mathbf{B}_{\text{Mod}}$  field in the  $0xy$  plane by  $\pi/2$  ( $X$ - $Y$ ).

The scheme with switching the direction of the modulating field to the opposite in a zero constant field is essentially identical to the scheme of the Hanle magnetometer, according to which SERF sensors are built, with the exception that in our experiment we use linearly polarized light. The signal arising in such a scheme when the  $\mathbf{B}_{\text{Offs}}$  field varies around zero value has a resonant shape (Hanle resonance), and is characterized by a width equal to the inverse time  $T_2$  [37]. We investigated this shape at different cell temperatures, magnetic field values and modulation parameters. Sinusoidal modulation of the fields in the  $X$  and  $Y$  coils with a shift of  $\pi/2$  (in other words, rotation of the modulating field in the  $0xy$  plane) with a frequency of 5 Hz and an amplitude of 2.5 nT (5 nT p-t-p) was used. The resonances were recorded by linearly sweeping  $\mathbf{B}_{\text{Offs}}$  in the  $0xy$  plane at a fixed value of the longitudinal field  $\mathbf{B}_z$ . The  $S_B$  signals were extracted by a lock-in amplifier at the field modulation frequency. Next, the obtained signals were approximated by Lorentz (dispersion) contours with an arbitrary phase. The results are presented in the next section.

### 3. Results

Fig. 2a shows examples of signal records obtained when switching the direction of the magnetic field  $\mathbf{B}_{\text{Mod}}$  ( $B_{\text{Mod}} = 5$  nT,  $B_{\text{Offs}} = 5$  nT). It is evident that the amplitude of the transient processes is determined by the direction of the bias field  $\mathbf{B}_{\text{Offs}}$  – it is minimal when  $\mathbf{B}_{\text{Offs}} \parallel x$ . Fig. 2b shows the relaxation times measured after the end of the transient (precession) period. The projection of the total field onto the bias field  $\mathbf{B}_{\text{Offs}}$  is plotted along the horizontal axis.

At high temperatures and pump intensities, the contribution of spin-exchange broadening to  $T_2$  can be reduced to almost zero, which is used by SERF sensors. However, as noted in the Introduction, it is not at all obvious that such a narrowing of the Hanle resonance will be observed in the case of alignment. Fig. 3 shows the results of the study of the near-zero-field resonance parameters at different cell temperatures. We varied the bias field to see an effect similar to the SERF effect. We introduced this field into the  $z$  channel to be able to rotate the sweep direction of the  $\mathbf{B}_{\text{Offs}}$  field in the  $0xy$  plane without breaking the symmetry of the system. When interpreting the results obtained, it should be kept in mind that in the absence of magnetic fields, the alignment is characterized by axial symmetry with respect to the direction of the vector  $\mathbf{E}$  [32], and all perpendicular directions are equal (Fig. 1c).

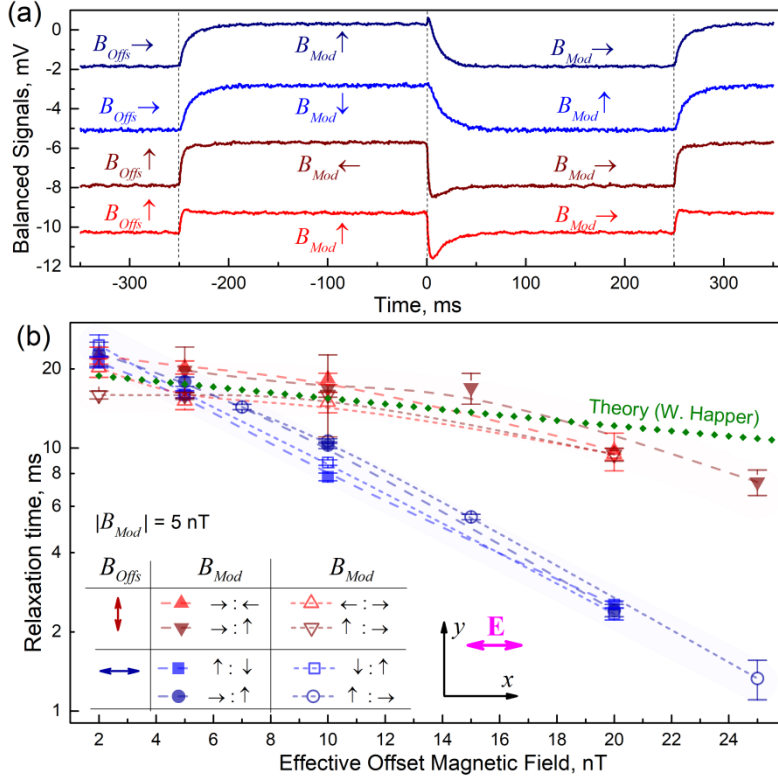


Fig. 2 (a) Examples of signal recordings during magnetic field switching ( $B_{Mod} = 5$  nT,  $B_{Offs} = 5$  nT). Arrows indicate the direction of the modulation magnetic field  $\mathbf{B}_{Mod}$  and the bias field  $\mathbf{B}_{Offs}$  in a given recording interval; (b) relaxation times measured after the end of the precession process and plotted against the projection of the total field onto the direction of the bias field  $\mathbf{B}_{Offs}$ . Dark green diamonds are the theoretical dependence of the SERF orientation resonance widths, calculated according to [37] (p.141).

It should also be noted that the shape of Hanle resonances at high temperatures can, according to [26,38], differ significantly from the classical one. We observed both the effects demonstrated in [26] (superposition of a second, narrower dispersion contour on a wide one) and others. Thus, in the inset in Fig. 3b, a partial reversal of the contour shape occurs, as a result of which it bifurcates, and the approximation yields the parameters of one of the two components – which is what causes the ultra-small widths of the resonance group (enclosed in a rectangle in Fig. 3b). The in-phase component of the signal (as well as its modulus) do not exhibit such features (which also correlates with the data in [26]).

#### 4. Discussion

To interpret the obtained results, we turn to the features of the formation of the alignment signal. The hodograph of the collective atomic moment in the case of pure alignment forms a symmetrical figure – either, depending on the alignment sign, a “barbell” or a “donut” [32,39]. Fig. 1c

schematically shows the dynamics of the alignment in the system with approximately equal relaxation times  $T_1 \approx T_2 \approx 1/\omega_L$  when the field  $B$  in the  $XY$  plane is switched on. Initially (in the absence of the field), the light creates alignment (let it be a “barbell”) in the direction of the vector of the electric component  $\mathbf{E} \parallel \mathbf{x}$ . As in the case of the “classical” Hanle effect in orientation, the result of the combined action of pumping, precession and relaxation is a turn of the ensemble, resulting in the appearance of non-zero alignment components along the  $y$  and  $z$  axes, and in a decrease in alignment along the  $x$  axis. The latter effect is detected by the pump beam. In this case, the transient processes caused by precession can significantly enhance the magnitude of the observed signals, which is observed in

Fig. 1b at sufficiently large fields. Note that the records in Fig. 1b, made with an  $X$ - $Y$  change in the field direction, are also characterized by a fast (compared to the times  $T_1$ ,  $T_2$ ,  $1/\omega_L$ ) jump associated with a change in the detecting properties of the radiation.

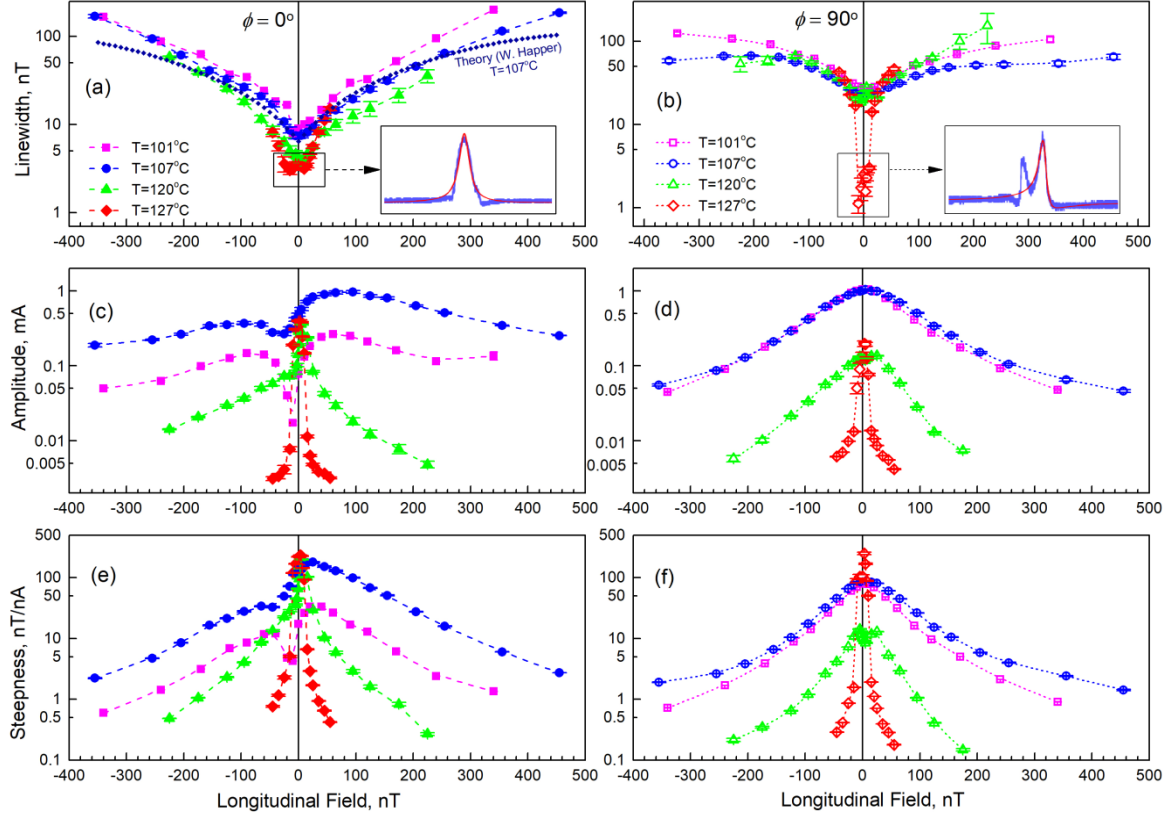


Fig. 3. Parameters of alignment signals under modulation and scanning of the transverse magnetic field depending on the values of the longitudinal field  $B_z$ : the left column is the component in-phase with the modulation, the right column is the quadrature component: (a), (b) are the resonance widths, (c), (d) are the amplitude, (e), (f) are the resonance steepness (the derivative with respect to the frequency offset at the line center). The rectangles highlight the points at which the quadrature components of the signals are characterized by an anomalous shape. Examples of signal records corresponding to such points are shown in the insets in (a), (b). The dark blue diamonds in (a) are the theoretical dependence of the SERF orientation resonance widths, constructed according to [37].

An analysis of the records presented in Fig. 2 shows that for  $B_{\text{off}} > B_{\text{Mod}}$  they can be divided into two groups corresponding to two directions of the  $\mathbf{B}_{\text{off}}$  field. The greatest degree of similarity of the records in the two groups is achieved if the effective offset field, i.e. the projection of the total field  $\mathbf{B} = \mathbf{B}_{\text{Mod}} + \mathbf{B}_{\text{off}}$  onto the  $\mathbf{B}_{\text{off}}$  direction (Fig. 2b), is plotted on the horizontal axis instead of  $\mathbf{B}_{\text{off}}$ . For comparison, Fig. 2b shows the theoretical dependence of the SERF orientation resonance width [18], constructed according to [37] (p.141) under the following conditions:  $T_c = 120^\circ\text{C}$ ,  $P_{N2} = 300$  torr,  $I_p = 5$  mW/cm<sup>2</sup>. It is evident that it qualitatively and quantitatively corresponds to the results we obtained for  $\mathbf{B}_{\text{off}} \parallel \mathbf{y}$ .

For  $\mathbf{B}_{\text{off}} \parallel \mathbf{x}$ , the dependence of the relaxation time on the bias field is much sharper. It is well described by the exponential  $T = T_0 e^{-B/B_0}$ , where  $T_0 = 32$  ms,  $B_0 = 7.8$  nT. Consequently, additional mechanisms are responsible for the destruction of the alignment under these conditions, which, according to [18], do not affect the orientation, and the rate of relaxation caused by them in ultra-weak fields

depends exponentially (and not quadratically, as in the usual SERF) on the field strength. This confirms the previously stated assumption that the law of conservation of angular momentum may not (or, more precisely, cannot) ensure the preservation of the alignment state. Note that in the  $\mathbf{B} \parallel \mathbf{x}$  and  $(\mathbf{B} \parallel \mathbf{y}, \mathbf{B} \parallel \mathbf{z})$  configurations, the selection rules for optical transitions are  $\Delta m_F = 0$  and  $\Delta m_F = \pm 1$ , respectively. Detailed schemes of transitions in Cs under pumping with linearly polarized light in transverse magnetic field are given in our previous work [34].

The maximum relaxation times recorded in our experiment are  $(25 \pm 2)$  ms, which corresponds to a resonance linewidth HWHM of 6.4 Hz. Recall that this is almost two orders of magnitude smaller than the magnetic resonance linewidth calculated without taking into account the SERF effect (approximately 1.6 kHz [37]). On the other hand, as follows from Fig. 2b, the times obtained in the experiment are in good agreement with the orientation resonance widths calculated taking into account the SERF effect. It should be noted here that in a zero field we also

practically do not see the effects of light broadening, which at a given intensity should be 10 Hz or more – most likely due to the effects of medium bleaching.

The next graph (Fig. 3) demonstrates that large relaxation times do correspond to ultra-narrow resonances that can be used in magnetometry. For clarity, one of the dependences shown in Fig. 3a is superimposed on the theoretical dependence of the width of the SERF orientation resonances, constructed according to [37] (p.141). It is evident that qualitatively (up to the uncertainty of the effective temperature in the cell, light broadening, gas pressure, etc.) it describes our results very well. Some asymmetry in the results may be due to both experimental errors (inaccurate alignment of the light polarization relative to the axis of the Helmholtz coils system, etc.) and light shifts.

The question may arise whether the signals recorded in our experiment are really alignment signals. Thus, in [39] it is shown that under certain conditions short-term dynamic effects lead to the conversion of alignment to orientation. Orientation, in turn, can cause circular birefringence and, as a consequence, rotation of the plane of polarization of the pump radiation. But the type of dependences of the obtained signals on the laser frequency confirms that they are linear dichroism signals – the maximum of their amplitude coincides with the peaks of the optical absorption profiles. This is also confirmed by the presence of  $S_T$  absorption signals, which cannot arise in the case of circular birefringence [34], and which in our experiment demonstrate the same dependences as the  $S_B$  signals in Fig. 3, although with a significantly lower signal-to-noise ratio.

Thus, it can be confidently stated that the SERF effect has been demonstrated in alignment. This effect provides some increase in the resonance steepness at high temperatures, and an even greater increase in sensitivity to magnetic field changes, taking into account the increase in absorption in the cell and the corresponding decrease in shot noise of light.

## 5. Conclusions

We have shown that transient processes occurring in the alignment under pumping with linearly polarized light and under switching of transverse magnetic fields are, under certain conditions, determined by longitudinal relaxation with a characteristic time  $T_1$ . We have also shown that, at sufficiently high temperatures and pump intensities, the contribution of spin-exchange broadening to the resonance width can be reduced practically to zero, much like in SERF sensors. This effect deserves further study, since the laws of conservation of angular momentum that determine the SERF effect in orientation, in our opinion, should not guarantee a similar effect in the alignment.

Indeed, in a bias magnetic field whose vector is directed along the vector of the electric component of light, the alignment relaxes significantly faster than the orientation

should relax. This, however, does not happen in the zero field, nor in the field applied in the perpendicular direction.

The results obtained are interesting from a theoretical point of view, and we hope that they will attract the attention of theoreticians. At the same time, they have specific practical significance, since they demonstrate the fundamental possibility of creating a compact SERF sensor based on the alignment effect in a single-beam scheme with a linearly polarized pump-detection beam and with balanced detection of the polarization rotation signal.

**Funding:** This research was funded by the baseline project FFUG-2024-0039 at the Ioffe Institute.

**Acknowledgments:** The authors thank Prof. Eugene B. Aleksandrov and Dr. Anatoly S. Pazgalev for valuable discussions.

**Conflicts of Interest:** The authors declare no conflicts of interest.

## References

- [1] S. Knappe, P. Schwindt, V. Shah, L. Hollberg, J. Kitching, L. Liew, and J. Moreland, A chip-scale atomic clock based on 87 Rb with improved frequency stability, *Optics Express* **13**, 1249 (2005).
- [2] J. Kitching, Chip-scale atomic devices, *Applied Physics Reviews* **5**, (2018).
- [3] D. Budker and M. Romalis, Optical magnetometry, *Nature Physics* **3**, 4 (2007).
- [4] M. V. Petrenko, A. S. Pazgalev, and A. K. Vershovskii, Single-Beam All-Optical Nonzero-Field Magnetometric Sensor for Magnetoencephalography Applications, *Phys. Rev. Appl.* **15**, 064072 (2021).
- [5] M. V. Petrenko, A. S. Pazgalev, and A. K. Vershovskii, All-Optical Nonzero-Field Vector Magnetic Sensor for Magnetoencephalography, *Phys. Rev. Appl.* **20**, 024001 (2023).
- [6] D. Meyer and M. Larsen, Nuclear magnetic resonance gyro for inertial navigation, *Gyroscopy and Navigation* **5**, 75 (2014).
- [7] A. K. Vershovskii, Yu. A. Litmanovich, A. S. Pazgalev, and V. G. Peshekhonov, Nuclear Magnetic Resonance Gyro: Ultimate Parameters, *Gyroscopy and Navigation* **9**, 162 (2018).
- [8] P. Neumann et al., High-precision nanoscale temperature sensing using single defects in diamond, *Nano Letters* **13**, 2738 (2013).
- [9] F. Dolde et al., Electric-field sensing using single diamond spins, *Nature Physics* **7**, 459 (2011).
- [10] E. Aleksandrov, A. Bonch-Bruevich, and V. Khodovoi, Possibilities for measuring weak magnetic fields by methods of optical orientation of atoms, *Opt. Spectrosc. (USSR)*, 23: 151-4 (Aug. 1967). (1967).
- [11] W. Franzen, Spin Relaxation of Optically Aligned Rubidium Vapor, *Phys. Rev.* **115**, 4 (1959).

- [12] M. Bouchiat and J. Brossel, Relaxation of optically pumped Rb atoms on paraffin-coated walls, *Physical Review* **147**, 41 (1966).
- [13] S. Appelt, A. Ben-Amar Baranga, A. R. Young, and W. Happer, Light narrowing of rubidium magnetic-resonance lines in high-pressure optical-pumping cells, *Phys. Rev. A* **59**, 2078 (1999).
- [14] M. P. Ledbetter, I. M. Savukov, V. M. Acosta, D. Budker, and M. V. Romalis, Spin-exchange-relaxation-free magnetometry with Cs vapor, *Phys. Rev. A* **77**, 033408 (2008).
- [15] I. K. Kominis, T. W. Kornack, J. C. Allred, and M. V. Romalis, A subfemtotesla multichannel atomic magnetometer, *Nature* **422**, 596 (2003).
- [16] T. Scholtes, V. Schultze, R. IJsselsteijn, S. Woetzel, and H.-G. Meyer, Light-narrowed optically pumped  $\{\mathbf{M}\}_x$  magnetometer with a miniaturized Cs cell, *Phys. Rev. A* **84**, 043416 (2011).
- [17] V. Schultze, B. Schillig, R. IJsselsteijn, T. Scholtes, S. Woetzel, and R. Stoltz, An Optically Pumped Magnetometer Working in the Light-Shift Dispersed Mz Mode, *Sensors* **17**, 3 (2017).
- [18] W. Happer and A. C. Tam, Effect of rapid spin exchange on the magnetic-resonance spectrum of alkali vapors, *Phys. Rev. A* **16**, 1877 (1977).
- [19] A. Ben-Kish and M. V. Romalis, Dead-Zone-Free Atomic Magnetometry with Simultaneous Excitation of Orientation and Alignment Resonances, *Phys. Rev. Lett.* **105**, 19 (2010).
- [20] H. Wang, T. Wu, W. Xiao, H. Wang, X. Peng, and H. Guo, Dual-Mode Dead-Zone-Free Double-Resonance Alignment-Based Magnetometer, *Phys. Rev. Applied* **15**, 024033 (2021).
- [21] C. Hovde, B. Patton, O. Versolato, E. Corsini, S. Rochester, and D. Budker, *Heading Error in an Alignment-Based Magnetometer*, in *Unattended Ground, Sea, and Air Sensor Technologies and Applications XIII*, Vol. 8046 (SPIE, 2011), pp. 184–189.
- [22] R. Zhang, D. Kanta, A. Wickenbrock, H. Guo, and D. Budker, Heading-Error-Free Optical Atomic Magnetometry in the Earth-Field Range, *Phys. Rev. Lett.* **130**, 153601 (2023).
- [23] M. Rosner, D. Beck, P. Fierlinger, H. Filter, C. Klau, F. Kuchler, P. Rößner, M. Sturm, D. Wurm, and Z. Sun, A highly drift-stable atomic magnetometer for fundamental physics experiments, *Applied Physics Letters* **120**, 161102 (2022).
- [24] A. Weis, G. Bison, and A. S. Pazgalev, Theory of double resonance magnetometers based on atomic alignment, *Phys. Rev. A* **74**, 033401 (2006).
- [25] A. Akbar, M. Kozbiál, L. Elson, A. Meraki, J. Kołodyński, and K. Jensen, *Optimized Detection Modality for Double Resonance Alignment Based Optical Magnetometer*, arXiv:2403.05357.
- [26] A. Meraki, L. Elson, N. Ho, A. Akbar, M. Kołodyński, and K. Jensen, Zero-field optical magnetometer based on spin alignment, *Phys. Rev. A* **108**, 062610 (2023).
- [27] G. Le Gal, G. Lieb, F. Beato, T. Jager, H. Gilles, and A. Palacios-Laloy, Dual-Axis Hanle Magnetometer Based on Atomic Alignment with a Single Optical Access, *Phys. Rev. Applied* **12**, 064010 (2019).
- [28] E. Breschi and A. Weis, Ground-state Hanle effect based on atomic alignment, *Phys. Rev. A* **86**, 053427 (2012).
- [29] M. T. Graf, D. F. Kimball, S. M. Rochester, K. Kerner, C. Wong, D. Budker, E. Alexandrov, M. Balabas, and V. Yashchuk, Relaxation of atomic polarization in paraffin-coated cesium vapor cells, *Physical Review A—Atomic, Molecular, and Optical Physics* **72**, 023401 (2005).
- [30] A. Omont, Irreducible components of the density matrix. Application to optical pumping, *Progress in Quantum Electronics* **5**, 69 (1977).
- [31] K. Blum, *Irreducible Components of the Density Matrix*, in *Density Matrix Theory and Applications*, edited by K. Blum (Springer, Berlin, Heidelberg, 2012), pp. 115–163.
- [32] D. Budker, D. F. Kimball, and D. P. DeMille, *Atomic Physics: An Exploration through Problems and Solutions* (Oxford University Press, USA, 2004).
- [33] W. Happer, Multipole relaxation times of a weakly perturbed spin system, *Physical Review B* **1**, 2203 (1970).
- [34] M. V. Petrenko, A. S. Pazgalev, and A. K. Vershovskii, A Method of Laser Frequency Stabilization Based on the Effect of Linear Dichroism in Alkali Metal Vapors in a Modulated Transverse Magnetic Field, *Photonics* **11**, (2024).
- [35] J. L. Margrave, Vapour Pressure of the Elements. By An. N. Nesmeyanov, Translated and Edited by JI Carasso, *Inorganic Chemistry* **3**, 1205 (1964).
- [36] A. Vershovskii, S. Dmitriev, and M. Petrenko, Spin-Exchange Broadening of the Magnetic MX Resonance in Cesium, *Technical Physics Letters* **47**, 421 (2021).
- [37] S. J. Seltzer, *Developments in Alkali-Metal Atomic Magnetometry*, Ph.D., Princeton University, 2008.
- [38] G. Di Domenico, G. Bison, S. Groeger, P. Knowles, A. S. Pazgalev, M. Rebetez, H. Saudan, and A. Weis, Experimental study of laser-detected magnetic resonance based on atomic alignment, *Phys. Rev. A* **74**, 6 (2006).
- [39] S. Rochester, M. Ledbetter, T. Zigdon, A. Wilson-Gordon, and D. Budker, Orientation-to-alignment conversion and spin squeezing, *Physical Review A—Atomic, Molecular, and Optical Physics* **85**, 022125 (2012).